1988

Condensation Heat Transfer of Binary Mixture Refrigerants of R22 and R114 Inside a Horizontal Tube

S. Koyama
Kyushu University

T. Fujii
Kyushu University

A. Miyara
Kyushu University

H. Takamatsu
Kyushu University

CONDENSATION HEAT TRANSFER OF BINARY MIXTURE REFRIGERANTS OF R22 AND R114 INSIDE A HORIZONTAL TUBE

Shigeru KOYAMA, Tetsu FUJII
Akio MIYARA and Hiroshi TAKAMATSU

Institute of Advanced Material Study, Kyushu University
6-1 Kasuga-shi, Fukuoka 816, Japan

Abstract

In recent years, increasing attention has been devoted to improving the thermodynamic performance of vapor compression heat pump systems by using nonazeotropic refrigerant mixtures as working fluid. In the development of the new system, accurate prediction of heat transfer characteristics in condensers and evaporators as well as thermodynamic properties of refrigerant mixtures is a requisite.

In the condensation of refrigerant mixtures inside a horizontal tube, there are a few studies reported in literatures[1-4]. However, more extensive work on the mechanism of the heat transfer is required because there are many possible combinations among components, mass fraction, heat transfer surface configuration and another factors.

The present paper deals with the experimental study on the condensation of the refrigerant mixtures of R22 and R114 inside a horizontal tube with internal spiral fins. The present results for heat transfer and pressure drop are compared with the previous studies on the condensation of pure refrigerants inside a horizontal smooth tube.

TRANSFERT DE CHALEUR PAR CONDENSATION DE MELANGES BINAIRES DE R22 ET R114 A L'INTERIEUR D'UN TUBE HORIZONTAL.

RESUME : Au cours des dernières années, on a porté de plus en plus d'attention à l'amélioration de la performance thermodynamique des pompes à chaleur à compression de vapeur, utilisant des mélanges de frigorigènes non azéotropiques. Dans la mise au point de nouveaux systèmes la prévision précise des caractéristiques de transfert de chaleur dans les condenseurs et les évaporateurs ainsi que des propriétés thermodynamiques des mélanges de frigorigènes est indispensable.

Quelques études ont été publiées sur la condensation des mélanges de frigorigènes à l'intérieur d'un tube horizontal. Cependant des travaux plus poussés sur le mécanisme de transfert de chaleur sont nécessaires parce qu'il y a de nombreuses combinaisons possibles des composants, de leur proportion massique, de la configuration de la surface de transfert de chaleur et d'autres facteurs.

Cette communication a trait à une étude expérimentale sur la condensation des mélanges de R22 et de R114 à l'intérieur d'un tube horizontal avec ailettes internes en spirale. Les résultats actuels du transfert de chaleur et de la chute de pression sont comparés avec ceux des études précédentes sur la condensation de frigorigènes purs à l'intérieur d'un tube lisse horizontal.

CONDENSATION HEAT TRANSFER OF BINARY MIXTURE REFRIGERANTS OF R22 AND R114 INSIDE A HORIZONTAL TUBE

Shigeru KOYAMA, Tetsu FUJII
Akio MIYARA and Hiroshi TAKAMATSU

Institute of Advanced Material Study, Kyushu University
6-1 Kasuga-shi, Fukuoka 816, Japan

EXPERIMENTAL APPARATUS AND MEASUREMENT

Figure 1 shows the schematic diagram of an experimental apparatus, which is a vapor compression heat pump loop composed mainly of 0.75 kW-closed type compressor 1, an oil separator 2, a test condenser 3, a subcooler 5, an expansion valve 7 and an evaporator 8. Heat source and heat sink units 12 and 13 are used to supply water at constant temperature to the evaporator and condenser, respectively. Refrigerant flow rate and pressure level in the loop are regulated by changing the speed of compressor and the opening of expansion valve. The pressure level can be also modified by changing the flow rate and/or temperature of water supplied to condenser and evaporator.

The schematic views of the test condenser and test tube are shown in Figs. 2 and 3, respectively. The test condenser is a tube-in-tube counterflow type condenser, where refrigerant flows inside the inner tube and heat sink water flows countercurrently in the outer annulus. The inner tube is made of copper with dimensions as follows: outer diameter 9.52 mm, mean wall thickness 0.60 mm, mean inner diameter 8.32 mm, fin hight 0.15 mm, number of fins 60, lead angle of fins 30 . The outer tube is made of polycarbonate resin with an inner diameter of 16 mm. The total length of the condenser is 4.8 m, and the outer annulus is subdivided into twelve sections in order to measure the local heat transfer characteristics, where the effective heat transfer zone in each section of 0.4 m in length is estimated to be 0.37 m in length.

The flow rates of refrigerant and heat sink water are measured by a turbine-type flow meter and a float-type flow meter, respectively, as shown in Fig. 1. The refrigerant temperature T_r, the temperature of heat sink water T_s and the vapor pressure P are measured at the inlet and exit of each section, and the circumferential temperature distribution on the outer surface of inner tube T_{wo} is measured at the central position of each section by 4 copper-constantan thermocouples, the hot junctions of which are located at the top, left side, right side and bottom, as shown in Fig. 2. The bulk mass fraction of refrigerant mixtures, which is sampled at the discharge port of compressor, is measured by a gas chromatograph.

Two kinds of pure refrigerants of R22 and R114 and three kinds of their mixtures containing about 25, 50 and 75 % bulk molar fractions of R114 were tested in the ranges of refrigerant mass velocity of 77 to 358 kg/(m^2 s) and condensing pressure of 0.3 to 2.1 MPa.

DATA REDUCTION

Fig.4 shows a physical model used to calculate the axial distributions of the vapor quality X, the saturation temperature T_{sat} and the vapor and liquid mass fractions of R114 $\bar{y}_V$ and $\bar{y}_L$ under the assumption that the radial distributions of temperature and concentration in the vapor layer can be ignored and those in the liquid film are also ignored. The energy balance during each section of Δz in length is expressed as

$$W_r \{(1-X_1)h_{L1} + X_1 h_{v1}\} - Q = W_r \{(1-X_2)h_{L2} + X_2 h_{v2}\} \quad (1)$$

where W_r is the mass flow rate of refrigerant, Q is the heat transfer rate calculated from the flow rate and temperature rise of heat sink water, h_v and h_L are the specific enthalpies of vapor and liquid, resectively, and the subscripts 1 and 2 denote the inlet and exit of each section , respectively. The vapor quality X is given by

$$X = (\tilde{y}_L - \tilde{y}_b) / (\tilde{y}_L - \tilde{y}_v) \quad (2)$$

where $\tilde{y}_b$ is the bulk mass fraction of R114. The local mass fractions $\tilde{y}_v$ and $\tilde{y}_L$ are determined from the phase equilibria expressed as

$$\tilde{y}_v = Y_v(P, T_{sat}) \quad (3)$$

$$\tilde{y}_L = Y_L(P, T_{sat}) \quad (4)$$

where P is the pressure. Specific enthalpy of vapor h_v is functionally expressed as

$$h_v = H_v(P, T, \tilde{y}_v) \quad (5)$$

where T_r is employed as T when $T_r \geq T_{sat}$, and T_{sat} is employed as T when $T_r < T_{sat}$. Specific enthalpy of liquid h_L is also expressed functionally as

$$h_L = H_L(P, T_{sat}, \tilde{y}_L) \quad (6)$$

where it is assumed that the effect of subcool of liquid is negligible. By solving the simultaneous equations composed of eqs. (1), (2), (3), (4), (5) and (6) under the conditions that X at the refrigerant inlet is equal to 1 and the measured data of W_r, P, Q and $\tilde{y}_b$ are given as known parameters, the axial distributions of X, T_{sat}, $\tilde{y}_v$ and $\tilde{y}_L$ can be obtained. The phase equilibria given by eqs. (3) and (4) and the thermodynamic properties given by eqs. (5) and (6) are calculated by the modified Benedict-Webb-Rubin equation[5], in which the value of interaction parameter among different kinds of molecules was settled to be 0.976 by refering to experimental data for thermodynamic properties of R22+R114[6].

Local heat transfer coefficient α is defined by

$$\alpha = q / (T_{sat} - T_{wi}) \quad (7)$$

with $q = Q / (\pi d_i \Delta z)$, $T_{wi} = \overline{T}_{wo} + Q \ln (d_o/d_i) / (2 \pi \Delta z \lambda_w)$

where q is the local heat flux density, d_i and d_o are the inner and outer diameters of test tube, respectively, $\overline{T}_{wo}$ is the arithmetic mean of four outer wall temperatures measured in each section, and λ_w is the thermal conductivity of tube wall. Average heat transfer coefficient $\overline{\alpha}$ is also defined by

$$\overline{\alpha} = \overline{q} / (\overline{T}_{sat} - \overline{T}_{wi}) \quad (8)$$

with $\overline{q} = W_r (h_{v,z=0} - h_{L,z=l}) / (\pi d_i l)$, $\overline{T}_{sat} = (T_{sat,z=0} + T_{sat,z=l}) / 2$, $\overline{T}_{wi} = (\Sigma T_{wi} \Delta z) / l$

where l is the total condensing length, the superscript $\bar{}$ denotes the mean value, and the subscripts $z=0$ and $z=l$ denote the refrigerant inlet and the position where the condensation has just completed, respectively.

Frictional pressure drop during each section ΔP_F is calculated by the following equation.

$$\Delta P_F = \Delta P_T - \Delta P_M \quad (9)$$

with

$$\Delta P_T = P_2 - P_1 \quad , \quad \Delta P_M = \left[\frac{G^2 X^2}{\xi \rho_v} + \frac{G^2 (1-X)^2}{(1-\xi) \rho_L} \right]_1 - \left[\frac{G^2 X^2}{\xi \rho_v} + \frac{G^2 (1-X)^2}{(1-\xi) \rho_L} \right]_2$$

where ΔP_T is the measured static pressure drop, ΔP_M is the pressure change due to the momentum change, G is the mass velocity of refrigerant, ρ_v and ρ_L are the densities of vapor and liquid, respectively, and ξ is the void fraction which was estimated by Smith equation [7].

In the dimensionless expression of local heat transfer coefficient and frictional pressure drop, the thermophysical properties of superheated vapor, saturated vapor and saturated liquid at each local position are used as reference properties. In the dimensionless expression of average heat transfer coefficient, the thermophysical properties of superheated and saturated vapors at the inlet of refrigerant and those of saturated liquid at the end point of condensation are used. The thermophysical properties of mixtures are estimated as follows : 1) the dynamic viscosity of liquid is calculated from the equation

expressed as $ln\ \mu_L = \Sigma y_{Li}\ (ln\ \mu_{Li})$, and that of vapor is calculated from the Wilke equation[8], 2) the thermal conductivity of liquid is calculated from the equation proposed by Chen et al.[9] and that of vapor is calculated from Wassiljewa equation[10] and Lindsay-Bromley equation[11], 3) both isobalic heat capacities of liquid and vapor are calculated from the equation expressed as $C_p = \Sigma\, y_i\, C_{pi}$.

RESULTS AND DISCUSSION

Local Heat Transfer

Fig. 5(a) and (b) show the examples of the experimental results for pure refrigerant R22 and refrigerant mixture 52mol%R22+48mol%R114, respectively, where the heat sink water temperature T_s, the inner wall temperature T_{wi}, the refrigerant temperature T_r, the saturation temperature T_{sat}, the function of vapor quality (1-X) and the heat flux density q are denoted by the symbols ○, □, △, ▽, ◇ and ●, respectively, and the section number used as an abscissa follows the order of distance from the refrigerant inlet. For pure refrigerant, superheated vapor entering the test section is cooled down to saturated vapor state with accompanying condensation and the condensation proceeds at almost constant temperature until condensation has completed. Then, the condensate is subcooled. Therefore, the temperature difference (T_{sat} - T_s) in the condensing region increases with the increase of the distance from the refrigerant inlet. The heat flux density q decreases in the flow direction of refrigerant in the superheated vapor condensation region and remains almost constant in the saturated vapor condensation region. For refrigerant mixture, on the other hand, the saturation temperature T_{sat} gradually decreases in the flow direction of refrigerant and the magnitude of the decrease depends on the bulk mass fraction. The heat flux density q also decreases in the flow direction of refrigerant. Forthermore, it is seen that the temperature difference (T_{sat} - T_s) can be kept almost constant during the condensing region by properly regulating the flow rates of refrigerant and heat sink water.

Figs. 6(a) and (b) show the axial distributions of the outer wall temperatures for pure R22 and mixtrue 52mol%R22+48mol%R114, respectively, where the temperatures measured at the top and bottom of the test tube are represented by the symbols ○ and □, respectively, and the temperatures at the right and left sides toward the flow direction of refrigerant are represented by the symbols △ and ▽, respectively. Figs. 6(a) and (b) correspond to the experiments shown in Figs. 5(a) and (b), respectively. For pure refrigerant, the circumferential temperature difference is small near the refrigerant inlet and gradually increases in the flow direction of refrigerant during condensing region. This reveals that the flow pattern near the inlet is annular flow like and changes into semi-annular flow like with condensation proceeding. In the semi-annular flow like region (6 to 9 Sec. no.), the wall temperature decreases circumferentially in the order of right side, top, bottom and left side. It is inferred from this fact that the liquid film is deformed circumferentially by the grooves cut like a right hand screw. For refrigerant mixture, on the other hand, the circumferential temperature distribution in the condensing region is small and does not changes in the flow direction of refrigerant. Tandon et al.[2] reported that the criteria to delinate different flow regimes for refrigerant mixtures are the same as those for pure refrigerants. It is inferred from the above mentioned facts that the temperature at the vapor-liquid interface changes circumferentially in the case of refrigerant mixtures. This also reveals that the mass transfer in the vapor layer is an important factor for the condensation of refrigerant mixtures.

Fig. 7 shows the comparison between the measured local Nusselt number $(Nu)_{exp}$ and the calculated values $(Nu)_{cal}$, which is estimated from an empirical equation for pure refrigerants inside a horizontal smooth tube[12]. The local Nusselt number is defined by $Nu = \alpha\, d_i / \lambda_L$, where λ_L is the thermal conductivity of liquid. The $(Nu)_{exp}$ values for R22 and R114 are higher than the $(Nu)_{cal}$ values by 40 — 70% and 50 — 80%, respectively. These facts reveal the effectiveness of condensation enhancement due to the internal spiral fins. The enhancement ratio $(Nu)_{exp}/(Nu)_{cal}$ for refrigerant mixtures is smaller than that for pure refrigerants and the axial variation of the ratio is affected by both the bulk concentration and flow rate of refrigerant.

Average Heat Transfer

Fig. 8 shows the comparison between the measured average Nusselt number for pure refrigerants and the following empirical equation, which was obtained for the condensation of pure organic substances inside a horizontal smooth tube by Fujii and Nagata[13].

$$\overline{Nu} = 0.25\ (l\ /\ d_i)^{-0.4}\ H^{-0.6}\ (Re_l\ Pr_L/R)^{0.8} \qquad (10)$$

where $\overline{Nu} = \overline{\alpha}\ l\ /\lambda_L$ is the average Nusselt number, $H = C_{pL}(\overline{T}_{sat} - \overline{T}_{wi})\ /\ (h_{vsat,z=0} - h_{Lsat,z=l})$ is the Phase change number, $Re_l = \rho_L U_v\ l\ /\mu_L$ is the two-phase Reynolds number, $R = \{\rho_L\ \mu_L/(\rho_v\ \mu_v)\}^{1/2}$ is the ρ-μ ratio, $Pr_L = \mu_L\ C_{pL}/\lambda_L$ is the Prandtl number of liquid, U_v is the mean vapor velocity at the refrigerant inlet, and the subscript sat denotes the saturated state. The measured values are about 100% higher than the values predicted by the equation (10). This proves that the internal spiral fins are effective in enhancing condensation. The experimental results for pure refrigerants can be correlated well by the following equation which is the same as eq. (10) except for a constant.

$$\overline{Nu} = 0.53\ (l / d_i)^{-0.4} H^{-0.6}\ (Re_l\ Pr_L/R)^{0.8} \qquad (11)$$

Fig. 9 shows the comparison between the experimental results for refrigerant mixtures and the equation (11). The data are lower than the values predicted by eq. (11). This reveals that the average heat transfer coefficients for refrigerant mixtures are lower than those for pure refrigerants.

Fig. 10 shows the relation between the ratio $(\overline{Nu})_{exp}/(\overline{Nu})_{cal}$ and bulk molar fraction of R114 y_b, where $(\overline{Nu})_{exp}$ is the measured value and $(\overline{Nu})_{cal}$ is the predicted value by eq. (11). The relation between $(\overline{Nu})_{exp}/(\overline{Nu})_{cal}$ and y_b can be approximated by the following equation.

$$(\overline{Nu})_{exp}/(\overline{Nu})_{cal} = f_y = 1 - 0.73\ y_b + 0.37\ y_b^2 + 0.36\ y_b^3 \qquad (12)$$

As shown in Fig. 11, the experimental data for pure and mixed refrigerants can be correlated well by the equation which was obtained by combining the eqs. (11) and (12).

Pressure Drop

Fig. 12 shows the examples of the results of pressure drop, where the closed and open symbols represent the measured static pressure drop ΔP_T and the calculated pressure change due to momentum change ΔP_M, respectively. The values of $|\Delta P_T|$ and $|\Delta P_M|$ increase with the increase of mass velocity G.

Fig. 13 shows the frictional pressure drop plotted on the coordinate of Φ_v vs X_{tt}, where the symbols ● and △ denote the present results and the previous study for the two-phase flow of R22 in a horizontal smooth pipe[14], respectively, and the soid line denotes Lockhart-Martinelli relation[15]. Figs. (a), (b), (c) and (d) correspond to the results of R22, R114, 75mol%R22+25mol%R114 and 25mol%R22+75mol%R114, respectively. The Lockhart-Martinelli parameters Φ_v and X_{tt} are defined by

$$\Phi_v = \sqrt{(\Delta P_F/\Delta z)_2/(\Delta P/\Delta z)_v}\ ,\ X_{tt} = \{(1 - X)/X\}^{0.9}\ (\rho_v/\rho_L)^{0.5}\ (\mu_L/\mu_v)^{0.1}$$

where $(\Delta P_F/\Delta z)_2$ is the frictional pressure gradient calculated from eq. (9) and $(\Delta P/\Delta z)_v$ is the pressure gradient if all the fluid flows in the tube as a vapor. It is seen that the present results for the relation between Φ_v and X_{tt} are not affected by the bulk concentration and are correlated well by Lockhart-Martinelli relation.

CONCLUSIONS

Experimental study of condensation of refrigerant mixtures of R22 and R114 inside a horizontal tube with internal spiral fins was carried out for a tube-in-tube counterflow type condenser in the ranges of refrigerant mass velocity of 77 to 358 kg/(m^2 s) and condensing pressure of 0.3 to 2.1 MPa. The conclusions obtained are as follows:

(1) It is graphically shown that the axial distributions of saturation temperature, heat flux density, etc. for the refrigerant mixtures are different from those for pure refrigerants.

(2) By comparing the local heat transfer coefficient measured with those predicted from an empirical equation for the condensation of pure refrigerants inside a horizontal smooth tube, it is revealed that the condensation is enhanced by internal spiral fins, and that the enhancement ratios of refrigerant mixtures are lower than those of pure refrigerants and the axial distribution of the ratio is affected by both the bulk concentration and flow rate of refrigerant.

(3) Average heat transfer coefficient for pure and mixed refrigerants can be correlated well by the equation obtained by combining eqs. (11) and (12).

(4) Frictional pressure drop was estimated from the measured static pressure. The relation between Φ_v and X_{tt} is independent of molar fraction and is correlated by the Lockhart-Martinelli relation.

ACKNOWLEDGMENT

This study was supported by the Grant-in-Aid of Scientific Research of the Ministry of Education, Science and Calture, Japan, and was also sponsored by Japanese Association of Refrigeration.

REFERENCES

(1) Bokhanovskiy, YU. G., Heat Transfer Soviet Research, 12-4(1980), 43.
(2) Tandon, T. N., Varma, H. K. and Gupta, C. P., Trans. ASME, J. Heat Transf., 107-2(1985), 424.
(3) Tandon, T. N., Varma, H. K. and Gupta, C. P., Int. J. Refrig., 9-3(1986), 134.
(4) Mochizuki, S. and Tominaga, M., Proc. of 24th National Heat Transf. Sym. of Japan 1887, Matuyama(1987), 209.
(5) Nishiumi, H. ans Saito, S., J. Chem. Eng. Japan, 8-5(1975), 356.

(6) Hasegawa, N., Uematsu, M. and Watanabe, K., J. Chem. Eng. Data, 30-1(1985), 32.
(7) Smith, S. L., Heat and Fluid Flow, 1-1(1971), 22.
(8) Wilke, C. R., J. Chem. Phys., 18 (1950), 517.
(9) Chen, Z. S., Fujii, T. and Fujii, M., Report of Research Institute of Industrial Science, Kyushu University, no. 82(1987), 173.
(10) Wassiljewa, A., Physik, Z., 5 (1904), 737.
(11) Lindsay, A. L. and Bromley, L. A., Ind. & Eng. Chem., 42 (1950), 1508.
(12) Fujii, T., Honda, H. and Nozu, S., Refrigeration, JAR, 55-627(1980), 3.
(13) Fujii, T. and Nagata, T., Report of Research Institute of Industrial Science, Kyushu University, no. 52 (1973), 35.
(14) Hashizume, K., Int. J. Multiphase Flow, 9-4(1983), 399.
(15) Lockhart, R. W. and Martinelli, R. C., Chem. Eng. Prog., 45-1(1949), 39.

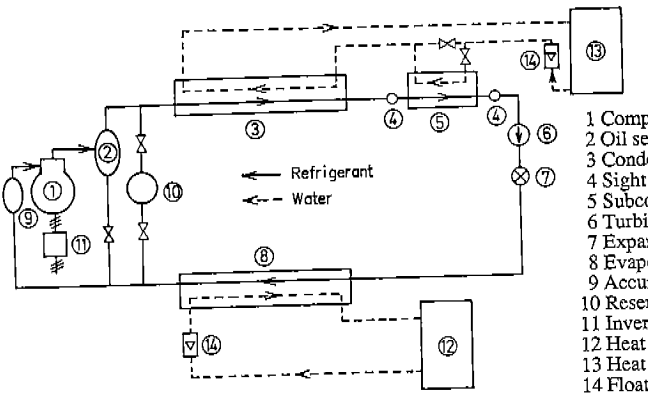

Fig. 1. Schematic diagram of experimental apparatus.

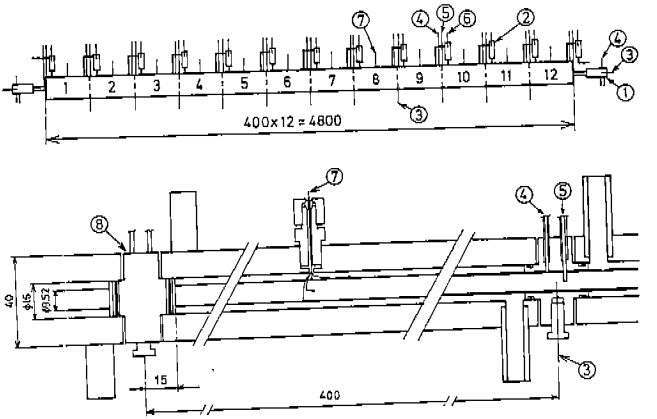

Fig. 2. Test condenser.

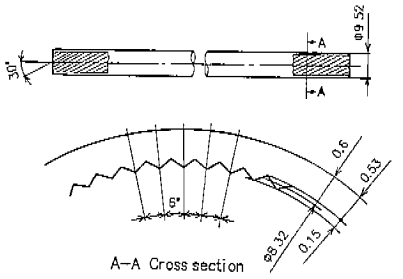

Fig. 3. Test Tube (inner tube).

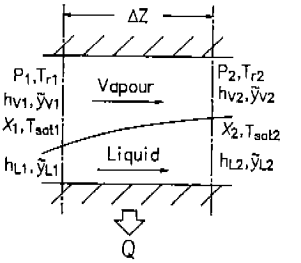

Fig. 4. Physical model.

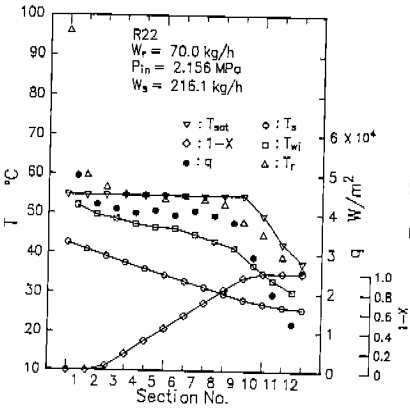

(a) R22

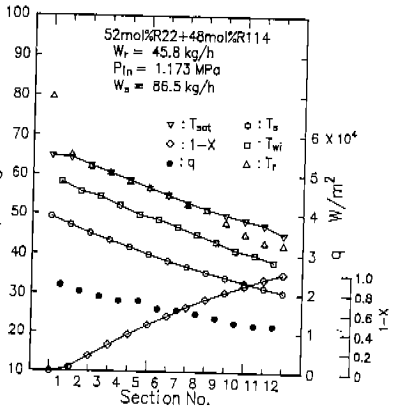

(b) 52mol%R22+48mol%R114

Fig. 5. Examples of experimental results.

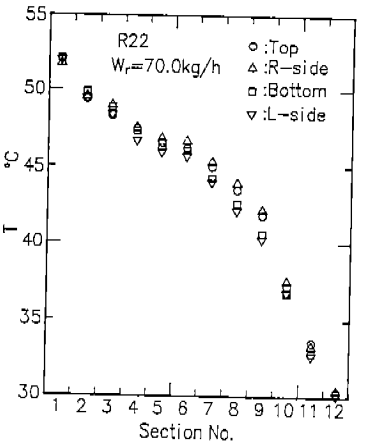

(a) R22

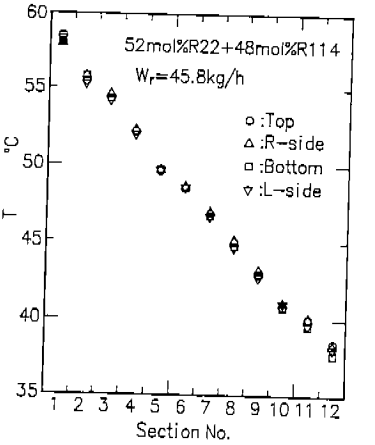

(b) 52mol%R22+48mol%R114

Fig. 6. Examples of axial distribution of tube wall temperature.

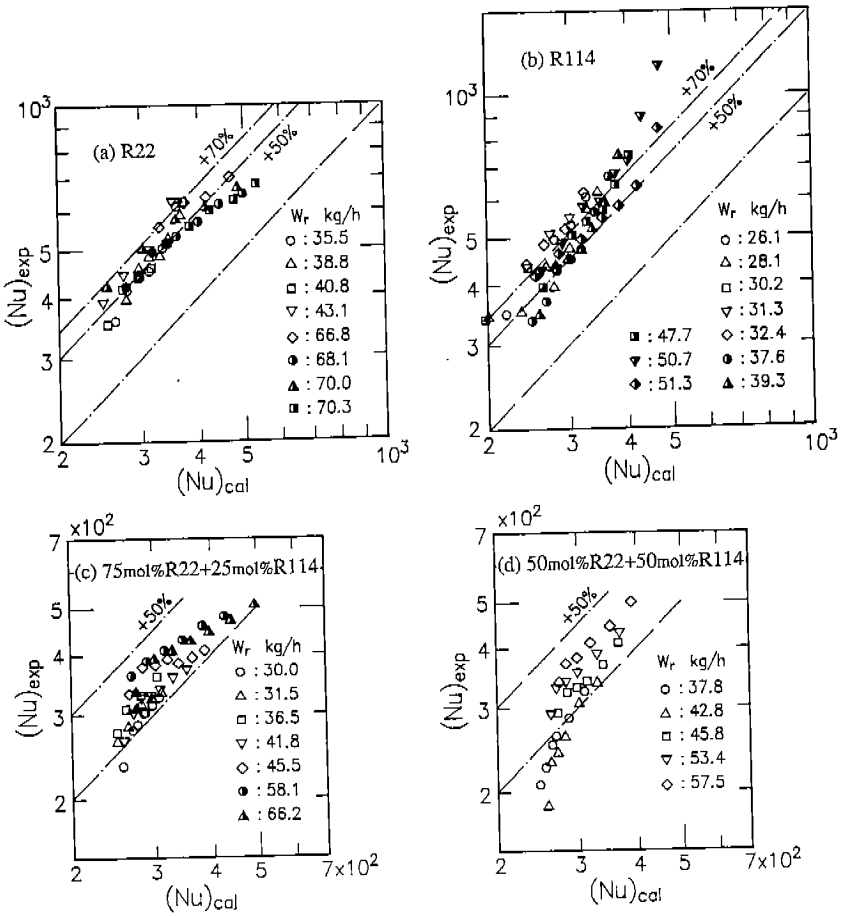

Fig. 7. Comparison between $(Nu)_{exp}$ and $(Nu)_{cal}$.

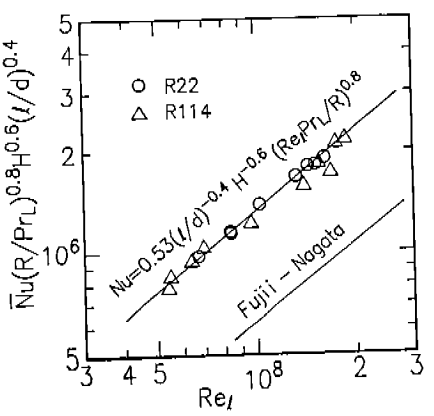

Fig. 8. Average Nusselt number (Pure refrigerants).

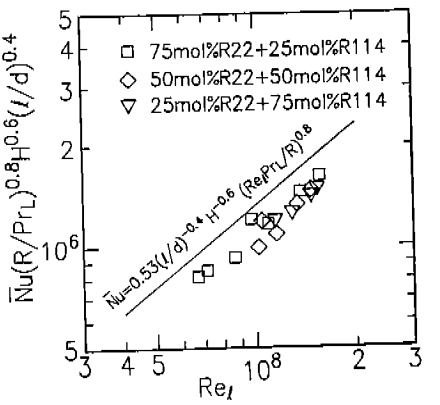

Fig. 9. Average Nusselt number (Refrigerant mixtures).

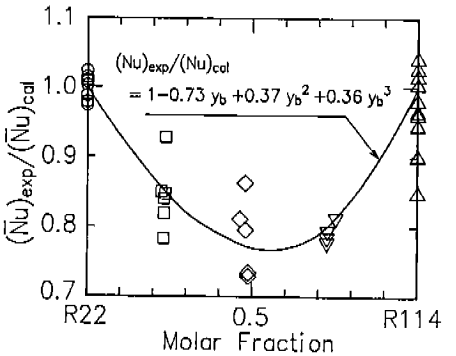

Fig. 10. Relation between $(Nu)_{exp}/(Nu)_{cal}$ and y_b.

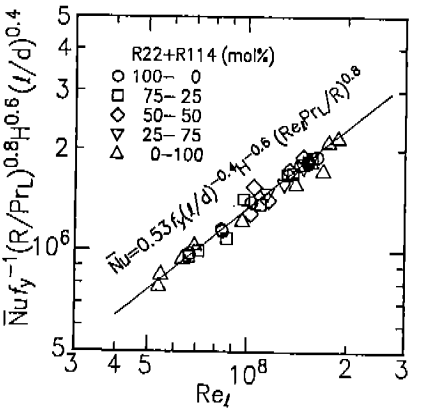

Fig. 11. Average Nusselt number of pure and mixed refrigerants.

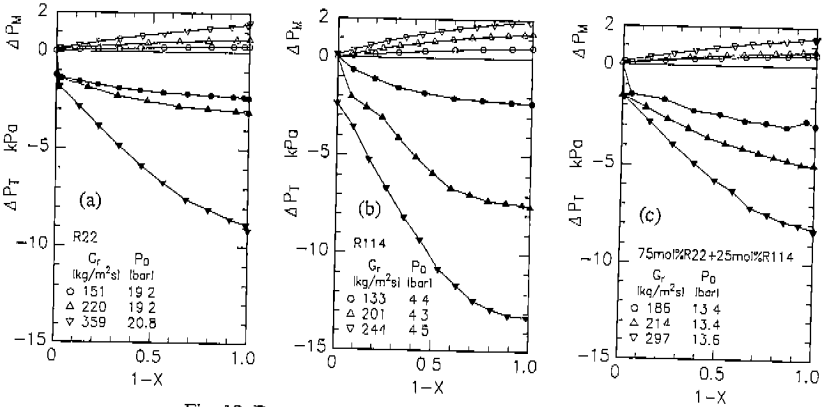

Fig. 12. Examples of axial distribution of pressure drop.

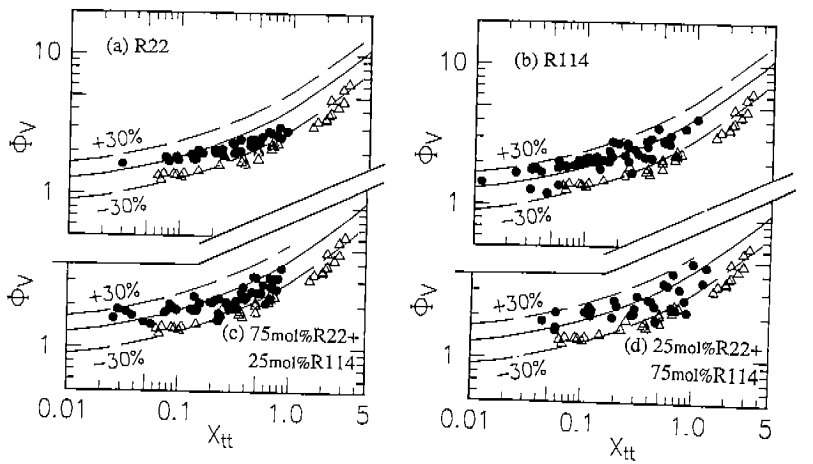

Fig. 13. Frictional pressure drop.